Vol. 15, No. 3 (2026): 1208 - 1221 http://dx.doi.org/10.23960/jtepl.v15i3.1208-1221

JURNAL TEKNIK PERTANIAN LAMPUNG

ISSN 2302-559X (print) / 2549-0818 (online)
Journal homepage : https://jurnal.fp.unila.ac.id/index.php/JTP

Performance of Shell Peeling Machine for Koro Pedang (*Canavalia ensiformis*)

Agus Sutejo[1,✉], Gilang Ramdani[1], Rafi Rizky Mulyadi[1], Dinur Saptiadi[1]

[1] Department of Mechanical and Biosystem Engineering, Faculty of Agricultural Technology, IPB University, Bogor, INDONESIA.

Article History:

Received : 20 October 2026
Revised : 27 February 2026
Accepted : 17 March 2026

Keywords:

Koro pedang bean,
Rotational speed,
Separation efficiency.
Shelling capacity,
Shelling machine.

Corresponding Author:
✉ agussutejo288@gmail.com
(Agus Sutejo)

ABSTRACT

The increasing demand for tempeh made from koro pedang (Canavalia ensiformis) beans requires large quantities of kernels processed rapidly and efficiently. This study evaluated the performance of a newly developed outer-shell peeling machine to enhance peeling capacity and seed–shell separation efficiency. Experiments were conducted at three rotational speeds (730, 820, and 960 rpm) with three replications per treatment. Observed parameters included peeling capacity, peeling efficiency, separation efficiency, percentage of broken seeds, and fuel consumption. Results showed that increasing rotational speed improved peeling capacity from 32.41 to 51.77 kg/h, with the highest value obtained at 960 rpm. Maximum peeling efficiency reached 93.09%, while the highest separation efficiency was approximately 83.09% at 960 rpm. The percentage of broken seeds remained low (≤0.99%). Fuel consumption was 0.43 L/h, indicating good energy efficiency for small- to medium-scale operations. Overall, the machine use increases production throughput, shortens processing time, and reduces reliance on manual labour, supporting the sustainable development of tempeh industries based on koro pedang beans.

1. INTRODUCTION

Koro pedang (*Canavalia ensiformis*) is a legume with long pod resembling a sword, and can be one of bean commodities having strategic potential in supporting diversification and substitution of soybeans in the national food system. Agronomically, koro pedang can grow at an altitude of up to 2000 m above sea level with an optimum temperature of 20–32 °C in tropical land and 14–27 °C in rainfed land, and rainfall of around 4200 mm/year (Safira *et al*., 2020), so that it has the potential to be widely developed in various regions of Indonesia. According to Wijaya & Suarna (2020), the fruit shape of the koro pedang is a pod that is large in size (30 cm length), with a yellowish-green color when it is young and brown when it is older. In terms of nutritional composition, koro pedang seeds contain about 66.1% carbohydrates, 27.4% protein, and 2.9% fat, with a relatively lower fat content compared to soybeans (Nazir, 2016). These characteristics make koro pedang suitable for developing as a raw material for various food products, including flour for cakes, cookies, and bakery products, as well as processed products such as crackers, nuggets, mayonnaise, and fermented ingredients for tempeh, tofu, soy sauce, and tauco (Widiantara, 2019). The production of tempeh using koro pedang beans has become a middle-to-lower industry that must be optimally utilized to improve the community's economy, especially in rural areas (Putra *et al*. 2021).

The koro pedang nuts, however, have not been used optimally in Indonesia because of anti-nutrient substances such as hemagglutinin, which must be processed first (Kusumawardhani, 2015). The optimization of the koro pedang faces obstacles in the post-harvest stage, especially the process of outer shelling and seed separation, which in many business units is still carried out manually, resulting in an impact on low production capacity, inconsistency in yield quality, as well as increased workload and risk of operator injury (Wulandari *et al*., 2021).

The use of outer shell peeling machines for legume pods needs to be expanded to make post-harvest processing easier and faster. According to Santoso *et al*. (2020), manual peeling of soybean outer shells with a wooden beater has proven to be ineffective because it takes a long time, large labor, and low working capacity. This emphasizes the urgency of using soybean outer husk peeling machines as a solution to replace inefficient manual methods and increase farmers' post-harvest productivity. According to Pratama & Abidin (2020), nut peeling needs to be done with the help of a machine with the aim of making the peeling process easier so that production efficiency and quality can be improved. Meanwhile, according to Radiansyah *et al*. (2020), the development of technology that is appropriate for the community, such as mung bean peeling machines, needs to be carried out so that the peeling process can be shorter. Sonda *et al*. (2019) also stated that a peeling machine is indispensable for farmers who cultivate bean commodities. These findings indicate that the adoption of peeling machines has become an important aspect of post-harvest mechanization for various legume crops. The application of such technology not only reduces dependence on manual labor but also increases processing capacity and operational efficiency. Therefore, the development and improvement of outer shell peeling machines are essential to support modern agricultural practices, enhance product quality, and increase the economic value of legume commodities.

Several previous studies have shown that the application of mechanization in the process of peeling bean commodities can increase efficiency and productivity. Al Faruuq & Mahmudi (2023) reported that the use of a peeling machine on peanuts can improve yield quality and speed up the process time. In addition, Cahyanto *et al.* (2019) showed that the regulation of the rotational speed and sieve amplitude in the mung bean peel separator machine was able to achieve separation effectiveness of up to 84.6%. However, these studies are still limited to commodities other than koro pedang and have not specifically examined the mechanical characteristics of different koro pedang seeds in the context of the peeling process. Furthermore, studies that quantitatively analyze the influence of rotational speed variations on key performance parameters, including peeling capacity, peeling efficiency, separation efficiency, seed damage rate, and fuel consumption in diesel motor-based engines for micro, small, and medium enterprises (MSMEs) are still very limited. In fact, these parameters are crucial in determining the technical feasibility and operational efficiency of a post-harvest technological innovation.

Based on these gaps, this study is designed to comprehensively analyze the effect of rotational speed variations on the performance of diesel-based koro pedang bean outer shell peelers. In particular, this study aims to evaluate peeling capacity, peeling efficiency, seed-husk separation efficiency, seed damage rate, and fuel consumption as indicators of operational energy efficiency. The results of this study are expected to make a scientific contribution in the form of a quantitative understanding of the relationship between operating parameters and machine performance in koro pedang commodities, as well as providing practical contributions in the form of recommendations for optimal operating conditions that apply to MSMEs to increase productivity, process efficiency, and strengthen the downstream of koro pedang commodities in a sustainable manner.

2. MATERIALS AND METHODS

2.1. Time and Place

This research will be carried out in July 2025. The identification of equipment and data collection of machine performance test data was carried out at PT Daud Teknik Maju Pratama, located in Cibereum Petir Village, Dramaga District, Bogor Regency, West Java. The material hardness test was carried out at the Food and Agricultural Product Processing Engineering Laboratory (TPPHP) of the Department of Mechanical and Biosystem Engineering. Meanwhile, data processing and thesis preparation were conducted at the Robotics and Control Instrumentation Laboratory in the Department of Mechanical and Biosystem Engineering, IPB University.

2.3. Tools and Materials

The tools and materials used for this study included a koro pedang bean peeling machine, measuring tape and rulers, rheometer, caliper, digital scale, stopwatch, tachometer, basins, trash bags, a grain moisture meter, stationery and computer, and koro pedang beans.

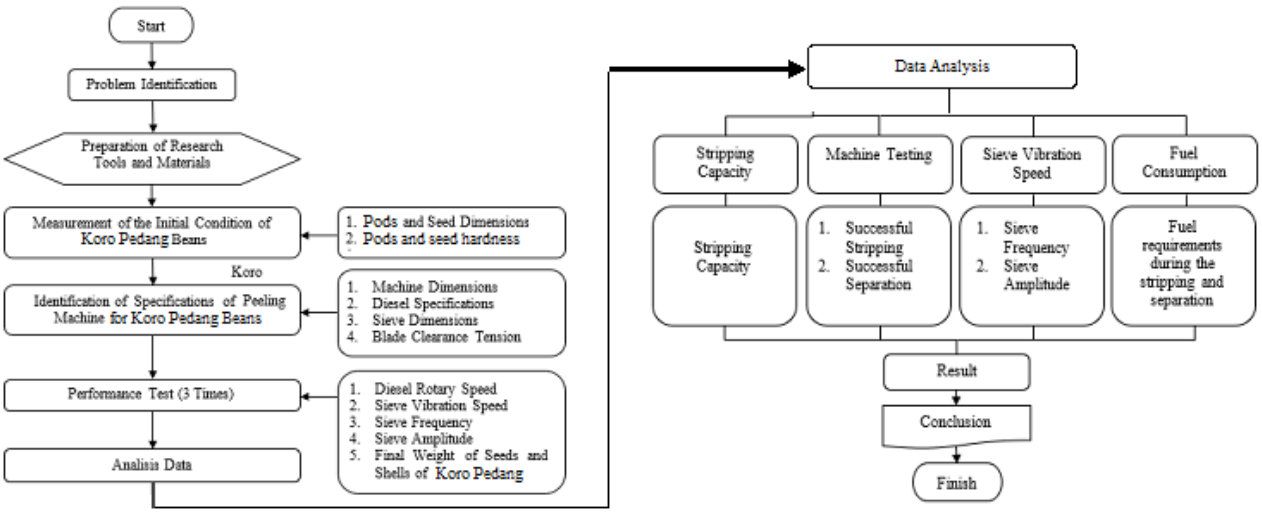

Figure 1. Research procedure flowchart

2.2. Research Procedure

The research procedure is shown in Figure 1. Three important steps involved preparation of tools and materials, equipment testing, data collection, and characterization of koro pedang beans.

2.2.1. Preparation of Tools and Materials

The purpose of preparing equipment is to minimize errors in the data collection process. In this step, koro pedang beans were prepared in appropriate quantities for preliminary research and machine performance testing. The machine along with the components was portrayed in Figure 2. The performance of machine involved parameters such as peeling capacity, yield of beans and shells, peeling efficiency, and engine fuel consumption.

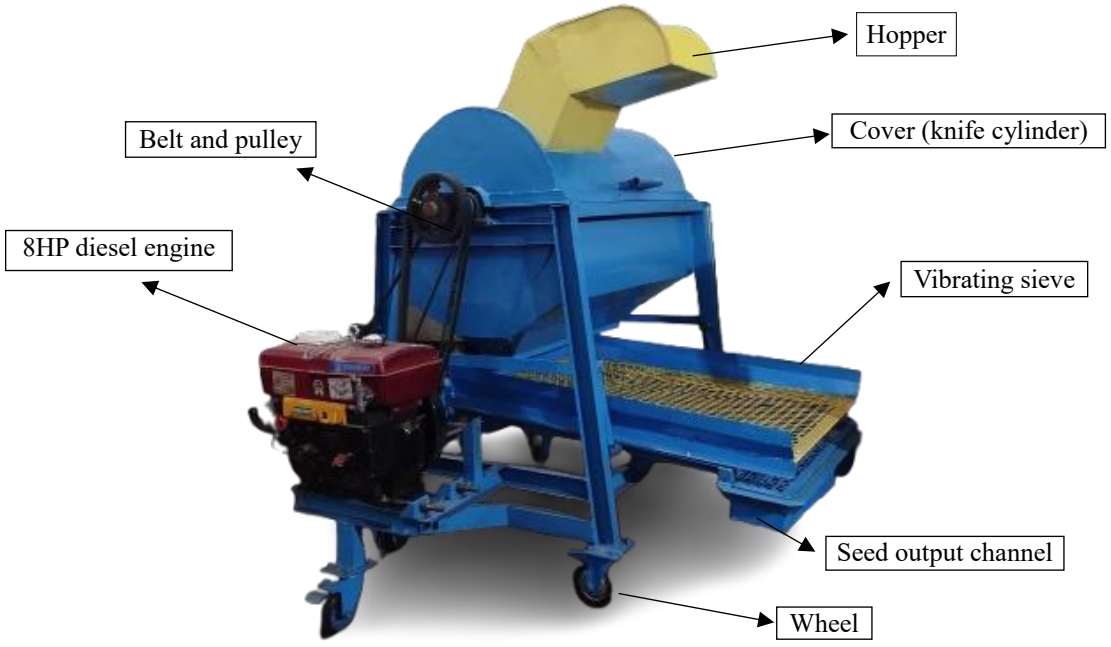

Figure 2. Peeling machine to remove outer shell of koro pedang beans

2.2.2. Equipment Performance Testing

The rotational speed variations evaluated in this study were 730, 820, and 960 rpm, each with three replications. These rotational speeds were selected based on preliminary testing and the stable operating range of the diesel engine and transmission system. The selected values represented low, medium, and high rotational-speed conditions while remaining within safe operational limits to avoid excessive vibration and mechanical loading on machine components. For each test, 1 kg of koro pedang material was used, resulting in a total material requirement of 9 kg. The peeling time was recorded after the material flow had reached a stable condition and the separation process through the vibrating sieve was operating normally. The collected data were analyzed to evaluate the peeling capacity, separation effectiveness, and fuel consumption at each rotational-speed variation.

2.2.3. Data Collection

Material characterization was conducted by measuring the dimensions and hardness of the pod skin and seeds of koro pedang using 10 randomly selected samples. Pod skin hardness was measured at several points on the surface to account for variation in material properties, whereas seed hardness was measured at one representative point for each sample. These measurements were conducted to determine the appropriate force and blade clearance required to remove the pod skin without causing damage to the seeds.

2.3. Characteristic of Koro Pedang Beans

The physical and mechanical characteristics of koro pedang included pod dimensions, seed diameter, seed length, seed colour, seed hardness, and moisture content, as presented in Figure 3. Seed diameter and length were measured using a Vernier calliper, whereas pod dimensions were measured using a ruler. Seed hardness was determined using a compression test with a rheometer at the Food and Agricultural Products Engineering Laboratory, Department of Mechanical and Biosystems Engineering, IPB University. The hardness value was calculated according to Equation (1).

$$H = F \cdot A \tag{1}$$

where H is hardness (kg/mm^2), F is maximum force (kg), and A is compressive cross-sectional area (mm^2).

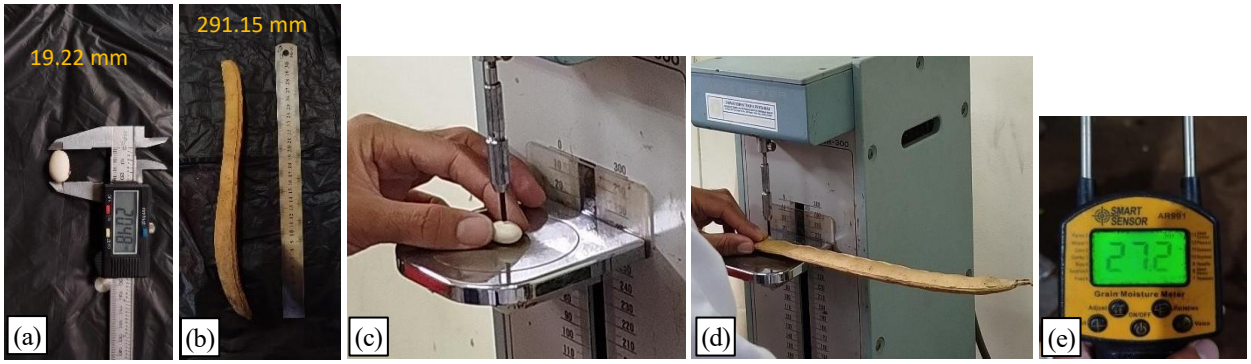

Figure 3. Measurement for: (a) bean length, (b) pod length, (c) bean hardness, (d) pod hardness, and (e) moisture content

2.4. Data Analysis

Data were analyzed using a descriptive quantitative approach. The machine performance data were processed numerically to provide an objective description of the machine performance without statistical hypothesis testing. The analyzed parameters included blade clearance, peeling capacity, peeling efficiency, separation efficiency, percentage of damaged seeds, percentage of pod skin and seeds retained on the sieve, sieve vibration frequency, and fuel consumption during the peeling process. The raw data were used to calculate the mean, percentage, and standard deviation for each parameter. The results were subsequently presented in tables and graphs to illustrate trends in machine performance, process efficiency, and the effects of operational parameters on the peeling and separation processes.

2.4.1. Calculation of fuel energy transfer rate

The peeling of koro pedang pods was performed using blades attached to a rotating shaft. The force generated by the blade clearance should be greater than the hardness of the pod skin but lower than the hardness of the seeds. This condition is necessary to ensure that the pod skin can be removed effectively while minimizing seed damage or deformation. According to Sularso & Suga (2004), the force acting on the rotating shaft blade can be calculated using Equation (2).

$$\tau = \frac{\sigma_B}{S_{f1} \times S_{f2}} \quad (2)$$

where τ is shear clearance voltage (kg/mm^2), σ_B is tensile strength of material (kg/mm^2), S_{f1} is safety factor 1, and S_{f2} is safety factor 2.

2.4.2. Peeling Capacity

Peeling capacity refers to the amount of material processed by the machine per unit time during the peeling operation. It was calculated by dividing the initial mass of the sample by the peeling time, following the method reported by (Cahyanto *et al.*, 2019). The peeling capacity was calculated using Equation (3).

$$P_c = \frac{m_0}{t} \quad (3)$$

where P_c is the peeling capacity (kg/s), m_0 is the initial mass of the sample (kg), and t is peeling time (s).

2.4.3. Peeling Success Rate

The peeling success rate represents the proportion of pods that were successfully peeled, resulting in the separation of seeds from the pod skin. It was calculated based on the mass of material that had been successfully peeled relative to the initial sample mass. The peeling success rate (P_{SR}) was determined using Equation (4).

$$P_{SR} = \frac{(m_0 - m_{BTK} - m_{KTK})}{m_0} \times 100\% \quad (4)$$

where m_{BTK} is the mass of unpeeled seeds, and m_{KTK} is the mass of unpeeled skin (g).

2.4.4. Separation Success Rate

The separation success rate indicates the percentage of pod components, including seeds and pod skin, that were successfully collected in their respective containers after passing through the separation system. The separation success rate (K_{PM}) was calculated using Equation (5). The unseparated material (K_{TM}) was calculated using Equation (6). Both are presented in %.

$$K_{PM} = \frac{B_P}{m_0} \times 100\% \quad (5)$$

$$K_{TM} = \frac{B_T}{m_0} \times 100\% \quad (6)$$

where B_P is the mass of pod material successfully collected in the designated container, including seeds and pod skin (g), and B_T is the mass of pod material that was not collected in the designated container, including seeds and pod skin (g).

2.4.5. Percentage of Pod Skin and Seeds Retained on the Sieve

The percentages of pod skin and seeds retained on the sieve were determined by comparing the mass of material retained on the sieve with the total mass of the corresponding material obtained after the separation process. Measurements were conducted for three replications, and the average values were used for further analysis. Equation (7) and (8) were respectively used to calculate the percentage of pod skin retained on the sieve (P_J) and seeds retained on the sieve (S_J).

$$P_J = \frac{m_{Kj}}{(m_{Kj} + m_{Kk} + m_{Kb})} \times 100\% \quad (7)$$

$$S_J = \frac{m_{\mathrm{Bj}}}{(m_{\mathrm{Bj}}+m_{\mathrm{Bk}}+m_{\mathrm{Bb}})} \text{ x } 100\% \quad (8)$$

where m_{Kj} is the mass of pod skin retained on the sieve (g), m_{Kk} is the mass of pod skin entering the pod-skin outlet (g), m_{Kb} is the mass of pod skin entering the seed outlet (g), m_{Bj} is the mass of seeds retained on the sieve (g), m_{Bb} is the mass of seeds entering the seed outlet (g), and m_{Bk} is the mass of seeds entering the pod-skin outlet (g)

2.4.6. Sieve Vibration Speed

The maximum vibration speed of the sieve is an important parameter in the separation process because it influences the acceleration and movement of pod skin and seeds across the sieve surface. The sieve vibration was generated by the rotation of an eccentric shaft connected to a pulley transmission system and driven by a diesel engine. The vibrating sieve moved in a reciprocating motion, producing vibrations that facilitated the separation of seeds from pod skin. The driving mechanism of the vibrating sieve consisted of belts, pulleys, shafts, an eccentric shaft, connecting rods, and the sieve frame. The maximum vibration speed was determined based on the vibration frequency and amplitude.

The vibration frequency was measured indirectly by determining the rotational speed of the eccentric shaft using a non-contact digital laser tachometer. Reflective tape was attached to the eccentric shaft, and the tachometer was directed toward the tape while the machine was operated at each rotational-speed treatment. Measurements were taken after the machine reached stable operating conditions. The measured rotational speed was then converted into vibration frequency. The vibration amplitude was measured as the maximum displacement of the sieve from its equilibrium position under stable operating conditions. Measurements were repeated several times to obtain representative average values. The vibration frequency and amplitude were subsequently used to calculate the maximum vibration speed (V_{max}) of the sieve using Equation (9).

$$V_{max} = 2 \times \pi \times f \times A \quad (9)$$

where f is sieve vibration frequency (Hz), and A is the vibration amplitude (m).

2.4.7. Fuel Consumption

Fuel consumption during the machine performance test was measured manually by recording the reduction in fuel volume in the fuel tank before and after each test. The fuel consumption rate was calculated by dividing the volume of fuel consumed by the operating time, as shown in Equation (10). The total fuel cost was calculated by multiplying the volume of fuel consumed by the fuel price per litre, as presented in Equation (11).

$$FCR = \frac{V_P}{t} \quad (10)$$

$$TFC = FP \times V_P \quad (11)$$

where FCR is the fuel consumption rate (L/h), V_p is the fuel consumption (L), t is the operating time for each treatment (h), TFC is the total fuel cost (IDR), and FP is the price for non-subsidized fuel (12,000 IDR/L).

2.4.8. Specific Fuel Consumption

Fuel consumption was measured at each engine rotational-speed variation by recording the volume of fuel consumed V_p (L) during a given operating time t (h). The hourly fuel consumption rate (FCR) was calculated using Equation (10). To provide a more representative evaluation of energy efficiency, fuel consumption was normalized against the peeling capacity and expressed as specific fuel consumption (SFC), with units of litres per kilogram of processed material (L/kg). The K_{ES} was calculated using Equation (12).

$$SFC = \frac{K_{BB}}{P_c} \quad (12)$$

This approach enabled a more comprehensive assessment of machine energy efficiency because fuel consumption expressed only in L/h does not reflect the amount of material processed. By normalizing fuel consumption per unit mass of processed material, the performance of different rotational-speed treatments could be compared more objectively.

3. RESULTS AND DISCUSSION

3.1. Characteristics of Pods and Beans of Koro Pedang

Characteristics of koro pedang pods generally contained approximately five to six seeds per pod. Based on measurements of 10 randomly selected samples, pod length ranged of 266.00–327.50 mm, while pod width and thickness ranged of 22.43–28.76 mm and 8.45–12.15 mm, respectively. The seeds ranged from 18.56 to 20.48 mm in length, 11.13 to 12.64 mm in width, and 7.97 to 9.18 mm in thickness. Table 1 presents the average dimensions of the pods and seeds.

Table 1. Size of seeds and pods of koro pedang beans

Sample	Length (mm)	Width (mm)	Thickness (mm)	Hardness (kg/mm^2)
Beans (Seeds)	19.22	12.03	8.72	19.82
Pods	291.15	25.52	10.67	--
Outer skin between seeds	--	--	--	3.93
Outer skin with seeds	--	--	--	8.78

In addition to physical dimensions, the mechanical properties of the material, particularly hardness, must be considered in the design of the peeling mechanism. Hardness testing is important to determine the resistance of agricultural materials to an applied load (Herlinawati, 2020). The hardness values of the pod skin and seeds were used as a basis for determining the appropriate blade force and clearance, so that the pod skin could be removed without causing seed damage. The hardness measurement is illustrated in Figure 3, while the results are presented in Table 1.

The compressive force measured using a rheometer was divided by the contact area to obtain the hardness value at each measurement point. The values obtained from several measurement points were averaged for each sample, and the mean values of all samples were subsequently calculated. The average hardness of the pod skin between the seeds was in average of 3.93 kg/mm². During the peeling process, pods may enter the machine in different orientations. Therefore, the hardness of the pod with seed was also measured because these parts may come into direct contact with the peeling blade. Based on measurements of three randomly selected samples, the overall average hardness of outer skin containing seed was 8.78 kg/mm².

The results presented in Table 1 indicate that the seeds had greater hardness than both the pod skin between seeds and the pod with seed. This finding was consistent with visual observations, which indicated that the seeds were mechanically more rigid than the pod skin. Differences in hardness between the pod skin and seeds may be influenced by differences in material structure and the compressive load applied during testing. Higher compressive forces may increase the measured resistance of a material, resulting in higher hardness values (Nariswara *et al*., 2013). The difference in hardness between the pod skin and seeds provides an important basis for determining the operating conditions of the peeling mechanism. The force generated by the peeling blade should exceed the hardness of the pod skin while remaining lower than the hardness of the seeds to ensure effective peeling without causing seed damage.

The moisture content of the pods was also measured before the peeling process using a grain moisture meter. Each sample was measured three times to improve data reliability. The moisture content was in average of 27.4%. This relatively high moisture content may influence peeling performance because wetter pod material tends to be more elastic, which may reduce the effectiveness of pod skin–seed separation. Documentation of the moisture-content measurement is presented in Figure 5. The grain moisture meter was used because of its practicality, rapid measurement capability, and availability at the test site. Although the gravimetric oven-drying method is widely recognized as a reference method for determining moisture content, it was not applied in the present study. Therefore, the reported moisture-content values should be interpreted as operational parameters for machine-performance analysis rather than absolute moisture-content values determined using a reference method. Future studies should validate the grain moisture meter against the gravimetric method to determine the agreement or correction factor between the two methods.

3.2. Determination of Experimental Treatments

Preliminary tests were conducted before the main experiment to evaluate the effects of rotational speed on machine performance. The rotational speed of the main shaft was adjusted by modifying the transmission ratio and engine speed.

The tested rotational speeds were 500, 600, 700, 800, 900, and 1,000 rpm. At 500 and 600 rpm, the torque generated by the machine was insufficient to produce adequate friction and impact forces for effective peeling. Under these conditions, peeling was incomplete and, in some cases, the engine stalled because it could not overcome the applied load. In contrast, operation at 1,000 rpm resulted in excessively high sieve vibration frequency and amplitude. This condition caused some stripped seeds to be thrown into the pod-skin container and resulted in structural instability, including detachment of the sieve arm from the main frame. Based on these observations, the rotational-speed range of 700–900 rpm was considered mechanically stable and safe for operation. Within this range, the machine operated without structural failure, the vibration level remained controllable, and peeling performance was acceptable. A feeding-capacity test was subsequently conducted to determine the appropriate initial mass of material for each test cycle, thereby preventing blockage and performance deterioration. The main experiment was therefore conducted under stable, safe, and technically controlled operating conditions.

3.3. Peeling Capacity

Appropriate postharvest technology is required to improve the efficiency and effectiveness of agricultural commodity handling (Sutejo & Prayoga, 2012). The peeling capacity of the machine increased with increasing rotational speed. At 730 rpm, the average peeling and separation time was 1.85 min, resulting in an average peeling capacity of 32.41 kg/h. At 820 rpm, the process required 1.33 min, with an average peeling capacity of 44.99 kg/h. At 960 rpm, the process time decreased to 1.15 min, resulting in the highest peeling capacity of 51.77 kg/h. These results indicate that increasing rotational speed reduced the processing time and increased peeling capacity. This trend is consistent with the findings of Wibowo *et al.* (2017), who reported that higher rotational speeds can accelerate the peeling process. Higher rotational speeds increase the movement of the blade shaft in the peeling chamber, thereby increasing the rate at which pods are conveyed and stripped. According to Muttaqin *et al.* (2023), traditional post-harvest handling of agricultural commodities relies heavily on limited human labours that is less effective and inefficient. The effect of rotational speed on peeling capacity is presented in Figure 4.

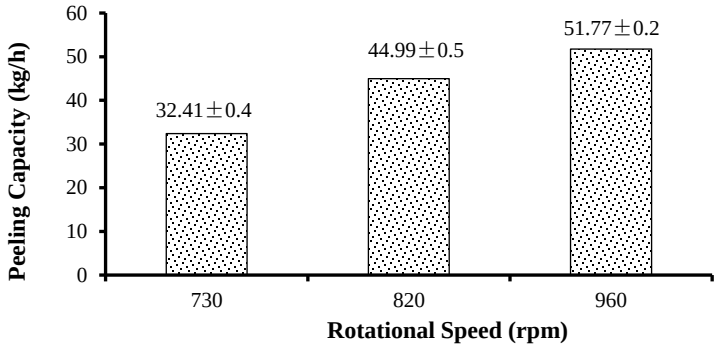

Figure 4. Effect of rotational speed on peeling capacity

Because the initial mass of material was constant for all treatments, peeling capacity was inversely proportional to processing time. Therefore, the shortest processing time at 960 rpm resulted in the highest peeling capacity. In contrast, the lowest capacity was obtained at 730 rpm. Rotational speeds below this range are not recommended because preliminary testing at 600 rpm showed that the diesel engine could not maintain its rotational speed when processing 1 kg of material and eventually stalled due to the increased load. Although higher rotational speed increased peeling capacity, the highest capacity does not necessarily represent the optimum operating condition. In a dynamic mechanical system, higher throughput must be evaluated together with vibration intensity, material losses, and structural loading. Therefore, peeling capacity was interpreted together with peeling efficiency, separation performance, material loss, and vibration stability to identify the most balanced operating condition.

Based on the information in Figure 4, the rotary speed will also affect the peeling capacity, which is affected by the process time. With the same amount of initial mass of material, the value of the peeling capacity is inversely proportional to the processing time, where the lower the peeling time, the greater the capacity. This indicates that the higher the

rotational speed, the greater the peeling capacity. The information in Figure 4 above shows that the highest peeling capacity is at a rotary speed of 960 rpm, and the lowest capacity is at a rotary speed of 730 rpm. Therefore, the recommended rotary speed for the peeling process is 960 rpm. The selection of a rotary speed that is too low is not recommended because preliminary research has been done on a rotary speed of 600 rpm. At that rotational speed, the diesel cannot maintain its rotational speed and dies. This happens when 1 kg of material enters the peeling tube. Diesel motors will bear more load, which causes a gradual decrease in rotational speed until the diesel dies.

Although the increase in rotary speed directly increases the peeling capacity, the maximum capacity does not automatically represent optimal operating conditions. In a dynamic mechanical system like this, increased throughput must be considered along with the potential for increased vibration, material loss, and dynamic load on the structure. Therefore, the capacity evaluation in this study was analyzed simultaneously with the parameters of efficiency, loss, and vibration stability to determine the most balanced operating range.

3.4. Peeling Performance

The peeling process occurred inside the peeling chamber using blades mounted on a rotating shaft. The shaft received rotational power from the diesel engine through a belt-and-pulley transmission system (Thoriq & Sutejo, 2017). The pulley diameter on the blade shaft was 8 inches, whereas the diesel-engine flywheel diameter was 4 inches. The pulley ratio influenced the rotational speed transmitted to the blade shaft. In general, pulley diameter and rotational speed have an inverse relationship, in which a smaller pulley rotates faster than a larger pulley under the same belt speed (Pane *et al*., 2023). Peeling performance was calculated as the proportion of pods that were successfully stripped relative to the initial mass of material. It was determined by subtracting the mass of unstripped material from the initial mass, dividing the result by the initial mass, and multiplying by 100%. The peeling-performance results are presented in Table 2, while the peeling condition at 960 rpm is illustrated in Figure 7. The results showed that the peeling percentage increased with increasing rotational speed. The highest peeling performance was obtained at 960 rpm. Higher rotational speeds increased the force exerted by the blade on the pods, resulting in more effective and uniform peeling. Consequently, a greater proportion of pod skin was removed at higher rotational speeds.

Table 2. Effect of rotational speed (rpm) on the average of peeling rate (%)

Rotary Speed (rpm)	Peeling Rate (%)	
	Peeled	Unpeeled
730	84.74	15.26
820	87.92	12.08
960	93.09	6.91

Table 3. Effect of rotational speed (rpm) on the average separation success percentage

Rotational Speed (rpm)	Separated (%)	Not Separated (%)	Loss
730	67.73	1.49	30.78
820	77.15	3.11	19.74
960	83.05	6.11	10.84

3.5. Separation Performance

The separation process was influenced by rotational speed. The separation-performance results are presented in Table 3 and Figure 5. At 730 rpm, 445.83 g of seeds entered the seed container, while 231.50 g of pod skin entered the pod-skin collection channel. At 820 rpm, the mass of seeds and pod skin successfully separated into their respective outlets increased to 466.13 g and 305.40 g, respectively. At 960 rpm, the highest masses of separated seeds and pod skin were obtained, reaching 490.77 g and 399.73 g, respectively. However, the mass of material that was not properly separated also increased at higher rotational speeds. At 960 rpm, 54.80 g of seeds and 6.33 g of pod skin were not separated correctly. At 820 rpm, the corresponding values were 26.60 g of seeds and 4.50 g of pod skin, whereas at 730 rpm, they were 12.30 g of seeds and 2.60 g of pod skin. The higher amount of unseparated material at high rotational speed was likely caused by excessive sieve vibration, which could throw seeds into the pod-skin container or cause material to move uncontrollably across the sieve surface. The results suggest that increasing rotational speed improved peeling and

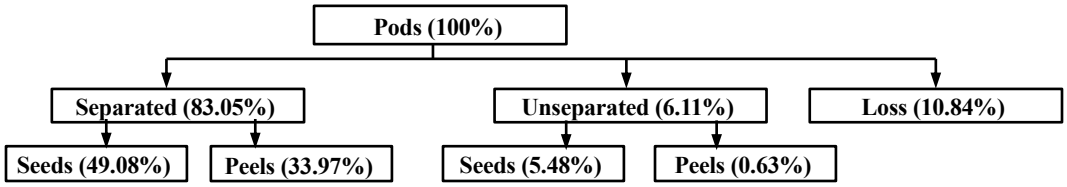

Figure 5. Separating performance of the machine for peeling of koro pedang pods at 960 rpm rotational speed

separation throughput by increasing the mechanical energy available to overcome the adhesion between the pod skin and seeds. However, the higher kinetic energy also increased the likelihood of particle rebound and uncontrolled movement within the sieve system. Thus, the optimum operating condition should be determined not only from the highest separation efficiency, but also from the balance between separation performance and minimization of product losses.

3.6. Percentage of Skins and Seeds Retained in the Sieve

A reciprocating sieve was used to separate pod skin from seeds. The sieve consisted of two layers. The first layer retained the larger pod-skin fragments, whereas the second layer directed the seeds toward the seed container. The first sieve layer had square openings of 4 cm × 4 cm. The second layer contained openings with a diameter of 0.75 cm, which functioned to prevent small pod-skin fragments that passed through the first layer from entering the seed outlet. At the end of the second sieve layer, a triangular seed outlet with sides of 3 cm directed the seeds to the collection container. Despite the sieve design, some pod skin and seeds remained trapped in the sieve. The quantities of pod skin and seeds retained on the sieve are presented in Figure 6. Pod-skin fragments were mainly retained in the openings of the first sieve layer, whereas seeds were generally trapped in the seed outlet channel (Figure 7).

The results showed a decreasing trend in the percentage of material retained on the sieve as rotational speed increased. At 730 rpm, the percentages of pod skin and seeds retained on the sieve were 59.51% and 15.93%, respectively. At 820 rpm, these values decreased to 27.76% for pod skin and 3.90% for seeds. At 960 rpm, the retained pod skin and seeds further decreased to 15.63% and 1.20%, respectively. The reduction in retained material can be attributed to the increased rotational speed of the diesel engine, which increased the rotational speed of the crankshaft and the frequency of sieve movement. Because the pulley diameter on the sieve-drive system was smaller than that of the diesel flywheel, the rotational speed of the sieve-drive shaft increased. Consequently, the reciprocating motion of the sieve became more frequent, facilitating the movement of pod skin toward the pod-skin outlet and seeds toward the seed outlet. However, higher vibration intensity may also increase the risk of material loss. Although faster sieve movement accelerated separation, excessive vibration could cause seeds to be thrown into an unintended outlet. This phenomenon indicates a trade-off between material-flow rate and separation selectivity.

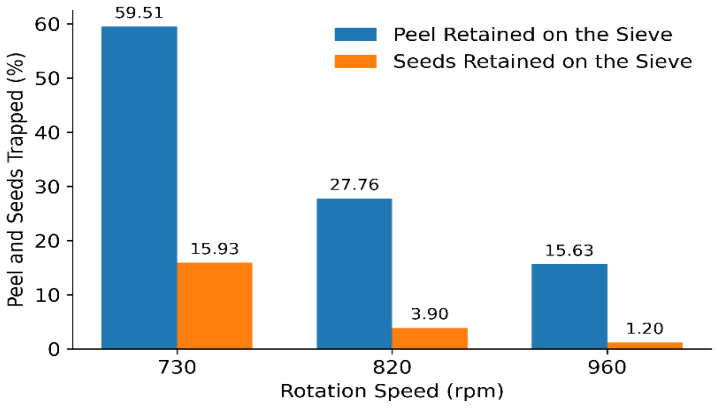

Figure 6. Relationship of rotational velocity to the skin and seeds retained in the sieve

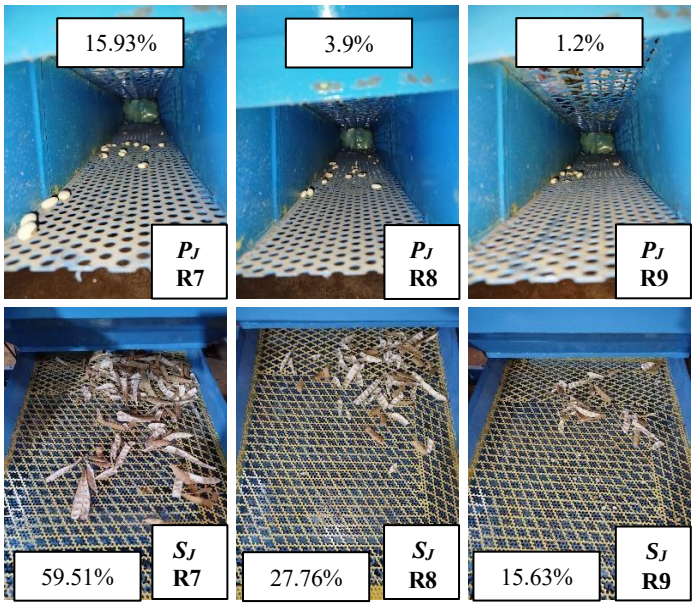

Figure 7. The seeds and skin stuck in the sieve (P_J = retained pod seeds, S_J = retained skin, R7, R8, R9 represent rotational speed of 730, 820, 960 rpm, respectively).

3.7. Sieve Vibration Speed

Sieve vibration speed is an important parameter affecting the performance of the mechanical separation system. The sieve motion can be described as oscillatory motion, which may be approximated using a simple harmonic motion model. According to Zhang *et al.* (2016), vibration speed is determined by two main parameters: frequency and amplitude. The vibration frequency was obtained from the rotational speed of the drive shaft, whereas the vibration amplitude was determined from the eccentricity of the sieve-drive shaft. The eccentricity represents the distance between the shaft centre and the connecting-rod attachment point. The relationship between diesel-engine rotational speed and sieve vibration speed is presented in Figure 8. The results showed a positive relationship between engine rotational speed and sieve vibration speed. The highest vibration speed was obtained at 960 rpm, reaching 1.99 m/s, whereas the lowest vibration speed was observed at 730 rpm, reaching 1.51 m/s. At 820 rpm, the vibration speed was 1.69 m/s. These results confirm that higher engine rotational speed increased the vibration speed of the sieve.

The vibration speed influenced the flow rate of pod skin and seeds toward their respective collection containers. The flow rates are presented in Table 5, whereas the relationship among rotational speed, sieve vibration speed, and material flow rate is illustrated in Figure 9. As vibration speed increased from 1.51 to 1.99 m/s, the pod-skin flow rate increased

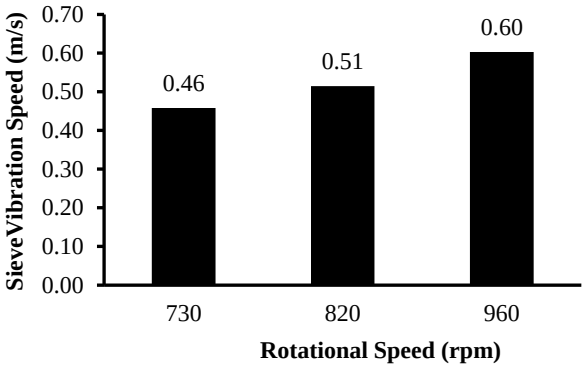

Figure 8. Relationship of rotational speed to sieve vibration

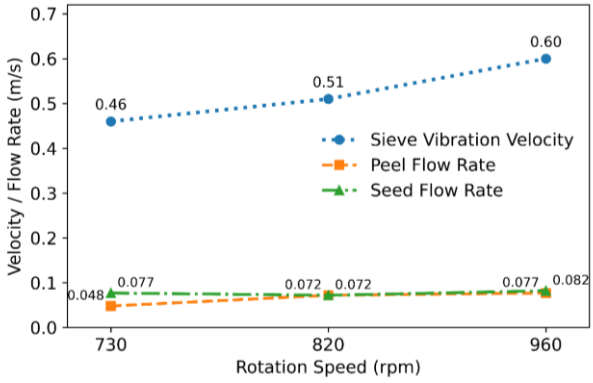

Figure 9. Relationship of vibrating speed to material flow rate

Table 5. Material flow rate in the vibrating sieve

Rotary Speed (rpm)	Sieve Vibration Speed (m/s)	Skin flow rate (m/s)	Seed flow rate (m/s)
730	0.46	0.048	0.077
820	0.51	0.072	0.072
960	0.60	0.077	0.082

from 0.048 to 0.077 m/s, while the seed flow rate increased from 0.077 to 0.082 m/s. The increase in material-flow rate can be explained by the greater acceleration and inertial force acting on the particles at higher vibration speeds, which accelerated material movement across the sieve surface (Singh & Heldman, 2014). However, the increase in seed-flow rate was less pronounced than that of pod skin, particularly at intermediate vibration speeds. This condition may be associated with temporary material accumulation, particle interactions, or flow resistance during the separation process. Therefore, the selection of an appropriate vibration speed is important because higher vibration speed may accelerate separation but can also affect flow stability and separation quality.

3.8. Fuel Consumption and Specific Energy Consumption

Fuel consumption was measured using a volumetric method by filling the fuel tank to a predetermined level and measuring the reduction in fuel volume after the completion of three replications for each rotational-speed treatment. Fuel consumption was measured for the complete set of replications rather than for individual runs to maintain stable engine operation during testing. The results showed that fuel consumption decreased as rotational speed increased, primarily because higher rotational speeds reduced the processing time. Fuel cost was calculated by multiplying the fuel volume consumed by the fuel price per litre. The fuel costs for each rotational-speed treatment and the total testing cost are presented in Table 6. Based on a non-subsidized fuel price of IDR 12,000/L, the fuel cost was IDR 2,520 at 730 rpm, IDR 840 at 820 rpm, and IDR 300 at 960 rpm, resulting in a total fuel cost of IDR 3,660 for the experiment. The fuel-consumption rate decreased from 2.27 L/h at 730 rpm to 0.43 L/h at 960 rpm.

Table 6. Fuel consumption cost of the koro pedang bean outer shell peeling machine

K_p (rpm)	V_p (L)	*t* (hour)	*FCR* (L/h)	*SFC* (L/kg)	*FP* (IDR/L)	*TFC* (IDR)
730	0.210	0.093	2.27	0.070	12,000	2,520
820	0.070	0.067	1.05	0.023	12,000	840
960	0.025	0.058	0.43	0.0083	12,000	300

Note: K_P = rotational speed, V_p = consumed fuel, *t* = peeling time, and *FCR* = fuel consumption rate, *SFC* = specific fuel consumption, *TFC* = total fuel cost.

Energy performance should not be evaluated solely based on hourly fuel consumption because this parameter does not account for the amount of material processed. Therefore, specific energy consumption was calculated by normalizing fuel consumption against peeling capacity. The specific fuel consumption (*SFC*) values were 0.070 L/kg at 730 rpm, 0.023 L/kg at 820 rpm, and 0.0083 L/kg at 960 rpm, as presented in Table 6. The reduction in specific energy consumption with increasing rotational speed indicates that the mechanical energy supplied by the system was used more effectively to produce peeling output. Higher rotational speeds increased the mechanical power transmitted to the peeling shaft and sieve system, thereby increasing peeling capacity. Because the output increased more rapidly than fuel consumption, the energy required per unit mass of processed material decreased. At 960 rpm, the machine achieved the lowest specific energy consumption and the highest peeling capacity. However, higher rotational speeds also increased sieve vibration intensity, which may increase structural loading and the risk of product loss due to more aggressive material movement. Therefore, the selection of the optimum rotational speed should not be based solely on the highest capacity or lowest specific energy consumption, but should also consider mechanical stability, material loss, and separation quality. Based on the overall results, the rotational-speed range of 700–900 rpm provided the most balanced operating condition in terms of energy efficiency, throughput, material-loss minimization, and system stability.

4. CONCLUSIONS AND SUGGESTIONS

Increasing rotational speed improved the performance of the koro pedang peeling machine. The peeling capacity ranged from 32.41 to 51.77 kg/h, with the highest capacity obtained at 960 rpm. At this rotational speed, the peeling efficiency reached 93.09%, the separation efficiency reached 83.05%, and fuel consumption was 0.43 L/h. Increasing rotational speed reduced processing time and increased machine capacity without substantially reducing separation performance. Although 960 rpm produced the highest peeling capacity and the lowest specific energy consumption, the overall selection of the operating speed should consider mechanical stability, material loss, and separation quality. The results indicate that a rotational-speed range of 700–900 rpm provides a more balanced operating condition for practical application, while 960 rpm may be considered when maximum throughput is the primary objective and the machine structure is sufficiently reinforced to withstand the increased vibration. The developed machine has potential for application in micro-, small-, and medium-scale enterprises involved in koro pedang processing. It may support increased production capacity, improved process consistency, and the development of koro pedang-based food products. Future studies should focus on improving the machine design, particularly by optimizing the sieve inclination, sieve-opening size, and transmission ratio through pulley-diameter modification to achieve more stable vibration. Further tests should be conducted using larger material capacities and under field operating conditions to evaluate performance consistency at the MSME scale. Additional studies should also assess energy efficiency, component wear, maintenance requirements, machine durability, ergonomics, and operator safety. Economic feasibility analysis, including investment cost, operating cost, and payback period, is also recommended to ensure that the machine is technically feasible, economically viable, safe, and sustainable for MSME-scale on koro pedang processing.

AUTHOR CONTRIBUTION STATEMENT

Author	C	M	So	Va	Fo	I	R	D	O	E	Vi	Su	P	Fu
AS	✓						✓					✓	✓	✓
GR			✓	✓	✓			✓						
RRM		✓				✓					✓			
DS									✓	✓				

C: Conceptualization	Fo: Formal Analysis	O: Writing - Original Draft	Fu: Funding Acquisition
M: Methodology	I: Investigation	E: Writing - Review & Editing	P: Project Administration
So: Software	D: Data Curation	Vi: Visualization	
Va: Validation	R: Resources	Su: Supervision	

REFERENCES

Al Faruuq, M.F., & Mahmudi, H. (2023). Analisa kebutuhan daya mesin pada alat pengupas kulit kacang tanah kapasitas 30 kg/jam. *Prosiding Seminar Nasional Inovasi Teknologi (SEMNAS INOTEK)*, ***7***(3), 1264–1274.

Cahyanto, D.D., Hendrawan, Y., & Djoyowasito, G. (2019). Kinerja pemisah kulit ari tauge kacang hijau (*Vigna radiata* L.) berdasarkan amplitudo ayakan dan variasi putaran. *Jurnal Keteknikan Pertanian Tropis dan Biosistem*, ***7***(3), 275–284. https://doi.org/10.21776/ub.jkptb.2019.007.03.08

Herlinawati, L. (2020). Mempelajari pengaruh konsentrasi maltodekstrin dan polivinil pirolidon (PVP) terhadap karakteristik sifat fisik tablet effervescent kopi robusta (*Coffea robusta* Lindl). *Agritekh (Jurnal Agribisnis dan Teknologi Pangan)*, ***1***(1), 1–25. https://doi.org/10.32627/agritekh.v1i01.17

Kusumawardhani, P.C. (2015). Pemanfaatan Kacang Koro Pedang (*Canavalia ensiformis*) Sebagai Bahan Substitusi dalam Pembuatan Tempe Kedelai. [*Undergraduate Thesis*]. Institut Pertanian Bogor.

Muttaqin, A.N., Mihdar, U.H., & Arfandy, A. (2023). Pengembangan mesin pemisah kulit polong kacang hijau untuk peningkatan kapasitas dan efisiensi pemisahan biji. *Machine: Jurnal Teknik Mesin*, ***9***(2), 51-57. https://doi.org/10.33019/jm.v9i2.4519

Nariswara, Y., Hidayat, N., & Effendi, M. (2013). Pengaruh waktu dan gaya tekan terhadap kekerasan dan waktu larut tablet effervescent dari serbuk wortel (*Daucus carota* L.). *Jurnal Industria*, ***2***(1), 27–35.

Nazir, A. (2016). Optimasi Produksi Benih Kacang Koro Pedang (*Canavalia ensiformis* L.) Melalui Pengaturan Pemangkasan dan Jarak Tanam. [*Undergraduate Thesis*]. Institut Pertanian Bogor.

Pane, A.H., Saputra, N., & Saktisahdan, T.J. (2023). Uji kerja mesin pencacah kulit kelapa berdasarkan perbedaan puli. *IRA Jurnal Teknik Mesin dan Aplikasinya (IRAJTMA)*, ***2***(2), 1–8. https://doi.org/10.56862/irajtma.v2i2.54

Pratama, O.A., & Abidin, Z. (2020). Perancangan mesin pengupas kulit kacang tanah home industri. *Jurnal Media Teknologi*, ***6***(2), 229-238.

Putra, I.A., Hasyim, A., Lubis, M.Z., Indah, M., Tanaji, I.P., Norcahyo, R., & Nugroho, S.S. (2022). Desain sistem pengupas kulit ari kacang koro pedang dengan tiga poros untuk pemberdayaan IKM di Kabupaten Gunung Kidul, Yogyakarta. In *Prosiding Simposium Nasional Rekayasa Aplikasi Perancangan dan Industri (RAPI XX 2021)*. Fakultas Teknik, Universitas Muhammadiyah Surakarta: 196–203.

Radiansyah, M., Murtadhahadi, & Arskadius. (2020). Rancang bangun mesin pengupas kulit polong kacang hijau sistem bantingan menggunakan motor listrik 1 HP. *Jurnal Mesin Sains Terapan*, ***4***(1), 29–36. http://dx.doi.org/10.30811/jmst.v4i1.1742

Safira, M.L., Kurniawan, H.A., Rochana, A., & Indriani, N.P. (2019). Pengaruh pemupukan nitrogen terhadap produksi dan kualitas hijauan kacang koro pedang (*Canavalia gladiata*). *Jurnal Nutrisi Ternak Tropis dan Ilmu Pakan*, ***1***(1), 25–33. https://doi.org/10.24198/jnttip.v1i1.25427

Santoso, E.B., Prastiyo, W.E., & Maulana, M.A. (2020). Rancang bangun mesin pengupas kulit luar kedelai dengan penggerak pedal. *CYBER-TECHN*, ***14***(2), 10-16.

Singh, R.P., & Heldman, D.R. (2014). *Introduction to food engineering* (5th ed.). Academic Press.

Sonda, L., Salam, A., Tangkemanda, A., Januar, R., & Aditya, A. (2019). Modifikasi mesin pemisah kulit polong kacang hijau. In Y.A.M.S. Yunus & Firman (Eds.), *Prosiding Seminar Nasional Penelitian & Pengabdian kepada Masyarakat (SNP2M) 2019*. Politeknik Negeri Ujung Pandang: 144–148.

Sularso, S., & Suga, K. (2004). *Dasar perencanaan dan pemilihan elemen mesin*. Jakarta: PT Pradnya Paramita.

Sutejo, A., & Prayoga, A.R. (2012). Rancang bangun alat pengupas kulit ari kacang tanah (*Arachis hypogaea*) tipe engkol. *Jurnal Keteknikan Pertanian*, ***26***(2), 107–114.

Thoriq, A., & Sutejo, A. (2017). Desain dan uji kinerja mesin pemarut sagu tipe TPB 01. *Agritech*, ***37***(4), 453–461. https://doi.org/10.22146/agritech.12789

Wibowo, D.H., Salahudin, X., & Widodo, S. (2017). Pengaruh kecepatan putar mesin pengupas kacang tanah tipe ruji vertikal terhadap kupasan. *Journal of Mechanical Engineering*, ***1***(1), 25–33. https://doi.org/10.31002/jom.v1i1.368

Widiantara, T. (2019). Pengaruh substitusi ubi jalar ungu (*Ipomoea batatas*) serta perbandingan kacang koro (*Canavalia ensiformis*) dengan susu skim terhadap karakteristik es krim. *Pasundan Food Technology Journal*, ***6***(1), 51–59. https://doi.org/10.23969/pftj.v6i1.1506

Wijaya, I.M.S., & Suarna, I.W. (2020). Karakter morfologis kacang pedang (*Canavalia gladiata* (Jacq.) DC.: Fabaceae) dan potensinya sebagai pakan ternak. *Pastura: Jurnal Ilmu Tumbuhan Pakan Ternak*, ***9***(2), 114–119.

Wulandari, W.S., Santosa, H., & Mulyono, J. (2021). Perancangan ulang alat pengupas kacang koro pedang rotaris disc dengan metode TRIZ. *Widya Teknik*, ***20***(2), 86–94.

Zhang, B., Gong, J., Yuan, W., Fu, J., & Huang, Y. (2016). Intelligent prediction of sieving efficiency in vibrating screens. *Shock and Vibration*, ***2016***, Article 9175417. https://doi.org/10.1155/2016/9175417